

# Initial development of the *urbisphere* urban hyperspectral library: Berlin, Germany

Giannis Lantzanakis  
Institute of Applied and Computational  
Mathematics, Remote Sensing Lab  
Foundation for Research and Technology  
Hellas  
Heraklion, Greece  
[lantzanakis@iacm.forth.gr](mailto:lantzanakis@iacm.forth.gr)

Dimitris Tsirantonakis  
Institute of Applied and Computational  
Mathematics, Remote Sensing Lab  
Foundation for Research and Technology  
Hellas  
Heraklion, Greece  
[dtsirantonakis@iacm.forth.gr](mailto:dtsirantonakis@iacm.forth.gr)

Nektarios Chrysoulakis  
Institute of Applied and Computational  
Mathematics, Remote Sensing Lab  
Foundation for Research and Technology  
Hellas  
Heraklion, Greece  
[zedd2@iacm.forth.gr](mailto:zedd2@iacm.forth.gr)

Sue Grimmond  
Department of Meteorology  
University of Reading  
Reading, UK  
[c.s.grimmond@reading.ac.uk](mailto:c.s.grimmond@reading.ac.uk)

Andreas Christen  
Environmental Meteorology  
University of Freiburg  
Freiburg, Germany  
[andreas.christen@meteo.unifreiburg.de](mailto:andreas.christen@meteo.unifreiburg.de)

Joern Birkmann  
Institute of Spatial and Regional Planning  
University of Stuttgart  
Stuttgart, Germany  
[joern.birkmann@ireus.uni-stuttgart.de](mailto:joern.birkmann@ireus.uni-stuttgart.de)

**Abstract**—The future sustainability of cities is linked directly with their adaptive capacity in response to both ongoing urbanization, weather extremes and climate change. Many possible actions are related to urban materials and their thermal and radiative properties. To explore alternatives using modelling and to monitor applications the thermal and radiative properties of materials are critical. However, there is a lack of hyperspectral data for a wide range of common materials. A Spectral Evolution RS-3500 spectroradiometer is used to measure 2151 spectral (1 nm) bands between 350 to 2500 nm in four representative neighborhoods of Berlin (Charlottenburg, Neukolln, Lichtenberg and Mitte) during August 2022. The data are processed to contribute 284 hyperspectral measurements of surfaces into the *urbisphere* hyperspectral library.

**Keywords**—*hyperspectral, spectral library, in-situ, RS-3500, spectroradiometer, vnir, swir, surface reflectance*

## I. INTRODUCTION

The resilience and adaptation strategies of cities in response to climate change are of practical and academic interest [1]. Many are linked to the urban materials. However, these are spatially variable with differing spectral radiation reflectances responses linked to material composition, structure, texture and other properties. As the spectral reflectance of urban materials affects energy exchanges and many other processes in cities, many applications (e.g., weather and climate modelling) are fundamental to energy-efficient building, neighbourhoods, cities and regions design. Spectral reflectance data are central to the mapping of urban surfaces and materials from satellite and aerial imagery.

Three examples of existing spectral reflectance libraries that have data for urban materials (e.g., asphalt, concrete, vegetation, and metallic surfaces) are:

- 1) Kotthaus et al.'s [2] undertook lab-based observations of 74 impervious urban materials to provide visible, near-infrared (VNIR) and short-wave infrared (SWIR) reflectance and a long-wave infrared (LWIR) emissivity.
- 2) The ECOSystem Spaceborne Thermal Radiometer Experiment on Space Station (ECOSTRESS) spectral library [3] aggregates data for 3000 natural and 72 artificial materials from laboratory observation for 0.35–15.4  $\mu\text{m}$  wavelengths.

- 3) Karlsruhe Library of Urban Materials (KLUM) provides 181 spectral signatures in the VNIR and SWIR spectral range, with a special focus on building façade materials viewed obliquely [4].

However, even combining these, the number of samples is very small for the variability of materials within each category (e.g., asphalt). Many factors impact surface reflectance, because of material composition linked to national/local regulations related to weather/climate conditions, local availability of raw materials and socio-economic factors.

To help address this data-gap, the *urbisphere* urban Hyperspectral (HS) library is being developed. This will use observations taken in several cities. Here, we focus on common materials found Berlin's (Germany) Charlottenburg, Neukolln, Lichtenberg and Mitte neighborhoods (Fig. 1). In August 2022 handheld spectroradiometer Spectral Evolution RS-3500 observations in the 350 to 2500 nm spectral region were undertaken. With 1 nm spectral resolution, this provides a total of 2151 spectral bands. Here, the methodology to acquire and process the data (Section II) are presented.

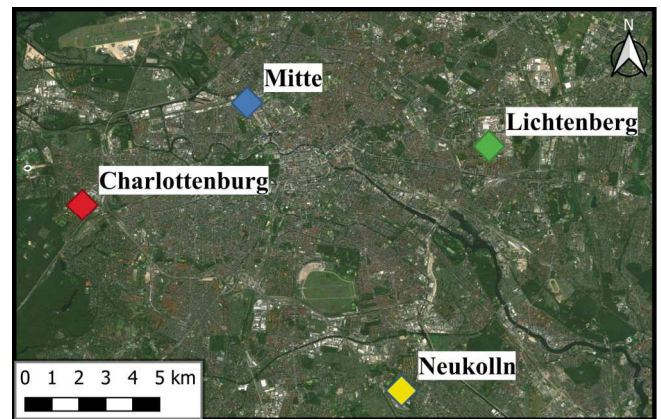


Fig. 1. Location of hyperspectral measurements in four neighborhoods of Berlin: (a) Charlottenburg, (b) Neukolln, (c) Lichtenberg and (d) Mitte.

## II. METHODOLOGY

### A. Sensor selection

The Spectral Evolution RS-3500 [5] is used for the *in-situ* HS measurements which provides high accuracy and

precision. It measures spectral radiation in a spectral range between 350 and 2500 nm using three sensors:

- 1) 512-element SI photodiode array (PDA) measures spectral radiation from 350 to 1100 nm with 2.8 nm spectral resolution at 700 nm. The sensor noise is  $0.008 \text{ mW m}^{-2} \text{ nm}^{-1} \text{ sr}^{-1}$ .
- 2) 256-element InGaAs measuring spectral radiation from 1101 to 1900 nm with 8 nm spectral resolution at 1500 nm. The sensor noise is  $0.012 \text{ mW m}^{-2} \text{ nm}^{-1} \text{ sr}^{-1}$ .
- 3) 256-element InGaAs measuring spectral radiation from 1901 to 2500 nm with 6 nm spectral resolution at 2100 nm. The sensor noise is  $0.018 \text{ mW m}^{-2} \text{ nm}^{-1} \text{ sr}^{-1}$ .

The combined measurements by the RS-3500 provide spectral signature with 1 nm spectral resolution, using spectral binning patterns [6].

### B. Field setup

As accurate measurements require a stable and powerful radiation source, cloud-free days with incoming solar radiation above  $200 \text{ W m}^{-2}$  are used. During this campaign this occurred 10:00 and 16:00 UTC.

Fig. 2 shows the measurement setup on an asphalt surface. with the tripod mounted RS-3500 optical fiber set at perpendicular distance  $\ell$  (0.20 m) from the target surface of interest. As the optical fiber has a Field of View (FOV) [7] of  $25^\circ$ , the diameter ( $d$ ) of the measurement area is 0.09 m:

$$d = 2\ell \cdot \tan\left(\frac{FOV}{2}\right) \quad (1)$$



Fig. 2. Measurement setup with a tripod mounted optical fiber 0.20 m above an asphalt surface, with the RS-3500 within the bag. (a) Incoming spectral radiation is estimated from measurements of the rectangular white Lambertian panel. (b) Outgoing spectral radiation is measured directly from the surface. The spectral reflectance (2) is the fraction of the outgoing radiation to the incoming radiation.

### C. Measurement retrieval principles

The RS-3500 measures the reflected spectral radiation,  $S(\lambda)$ , from the target, for each for wavelength,  $\lambda$ . To calculate the surface spectral reflectance,  $r(\lambda)$ , [8]:

$$r(\lambda) = \frac{S_t(\lambda)}{S_l(\lambda)} = \frac{S_t(\lambda)}{S_l(\lambda)/SRF_L(\lambda)} \quad (2)$$

both the spectral incoming,  $S_t(\lambda)$ , and outgoing  $S_l(\lambda)$  radiation are needed [8]. The latter is measured directly by the RS-3500 (Fig. 2b).  $S_t(\lambda)$  is estimated using the spectral reflected radiation  $S_l(\lambda)$  measured from the 0.12 m x 0.12 m Lambertian white panel (Fig. 2a) with its provided calibration factor,  $SRF_L(\lambda)$ .

The wavelengths of the measured spectra with strong atmospheric absorption (i.e. incoming solar radiation close to zero) are not analysed [9] resulting in gaps in the spectra (e.g., Fig. 3) at: 1345–1475 nm, 1780–2025 nm and 2340–2500 nm.

As the absorbed wavelengths differ with variations in the atmospheric composition [8], they can vary with geographic regions and time (e.g., date).

The RS-3500 has a maximum sample rate of 10 Hz and a default sample size of 10. As these settings caused instrument overheating and affected the spectra, we select a sampling rate of 1 Hz to measure the spectral reflected radiation for 5 samples after testing various settings as the optimum for accurate measurements.

As the sensor only saves the 5-sample mean spectral radiation,  $S^{(k)}(\lambda)$ , each point measurement ( $k$ ) is repeated five times to remove measurements impacted by external factors (e.g., cirrus cloud, passing car/humans). To identify the source of the measurement variability to be removed, the standard deviation (STD) is calculated for each measurement:

$$STD(\lambda) = \sqrt{\frac{1}{5} \sum_{k=1}^5 (S^{(k)}(\lambda) - \bar{S}(\lambda))^2} \quad (3)$$

where  $S(\lambda)$  is either the reflected spectral radiation from the target material or the Lambertian surface and  $\bar{S}(\lambda)$  the respective mean reflected spectral radiation. For each the mean coefficient of variation (COV) is obtained:

$$\frac{1}{(\lambda_n - \lambda_1 + 1)} \sum_{\lambda=\lambda_1}^{\lambda_n} \frac{STD(\lambda)}{\bar{S}(\lambda)} \leq 0.03 \quad (4)$$

where  $\lambda_1$  is the sensor's shortest wavelength and  $\lambda_n$  the longest. Valid measurements require the mean COV  $< 0.03$  for all three sensors.

The mean spectral reflectance  $\bar{r}(\lambda)$  is calculated as:

$$\bar{r}(\lambda) = \frac{\frac{1}{N_1} \sum_{n=1}^{N_1} (\bar{s}_\downarrow^{(n)}(\lambda))}{\frac{1}{N_2} \sum_{m=1}^{N_2} (\bar{s}_L^{(m)}(\lambda)/SRF_L(\lambda))} \quad (5)$$

where  $N_1$  and  $N_2$  are the total number of the remaining valid spectra, for the target and Lambertian surface respectively. To smooth residual noise the Nadaraya-Watson Regression with Radial Base Function (RBF) Kernel [10] is applied to the mean HS reflectance signatures calculated in (5). The smooth mean spectral reflectance,  $\bar{r}(\lambda)$ , is obtained from:

$$\bar{r}(\lambda) = \frac{\sum_{w=\lambda_1}^{\lambda_N} \left( \frac{1}{\sqrt{2\pi}} e^{-0.002|\lambda-w|^2} \bar{r}(w) \right)}{\sum_{w=\lambda_1}^{\lambda_N} \left( \frac{1}{\sqrt{2\pi}} e^{-0.002|\lambda-w|^2} \right)} \quad (6)$$

### D. Library classification

Each HS library spectrum has the following metadata associated with them:

- Cluster:* - A group of HS measurements with similar spectra.
- material name – e.g., asphalt, concrete, metal, grass
  - color – e.g., red, green, blue, yellow, orange, black
  - structure – e.g., smooth, fine roughness, porous
  - Status – e.g., new, weathered, dusty, rusty
  - usage – e.g., external wall, roof, ground, window

For example, Fig. 3 shows the HS measurements for the cluster labeled as: “Blue Smooth Ceramic Tile (Usage: External Wall)”. The cluster contains 8 HS measurements acquired at different locations within Berlin. Fig. 3 also shows the HS reflectance signatures for all the measurements within this cluster, while the picture corresponds to the 6<sup>th</sup> measurement. Apart from the unique denomination, each

cluster is also assigned a unique ID consisting of 13 alphabetical characters, the first and second representing the Material Type, third and fourth material's usage, fifth and sixth the color, seventh and eighth the structure, ninth and tenth the status, and the last three the location of the measurements. For example, for “Blue Smooth Ceramic Tile (Usage: External Wall)” the unique ID is “CC-EW-BL-SM-NO-BER”, where the digits: “CC” for Ceramic Tile, “EW” for External Wall, “BL” for blue color, “SM” for smooth, “NO” for Not-Specified (not a given status for this material), “BER” for Berlin. Each measurement included in a cluster of the HS library contains its own spectral reflectance, spectral incoming and reflected radiance, picture, geo-location (latitude and longitude), local time and a unique measurement ID. The unique measurement ID is 15 characters long and it is a combination of the cluster's ID and the measurement's index inside this cluster. For example, the picture in Fig. 3 belongs to the 6<sup>th</sup> measurement in cluster, with ID: “CC-EW-BL-SM-NO-BER-06”.

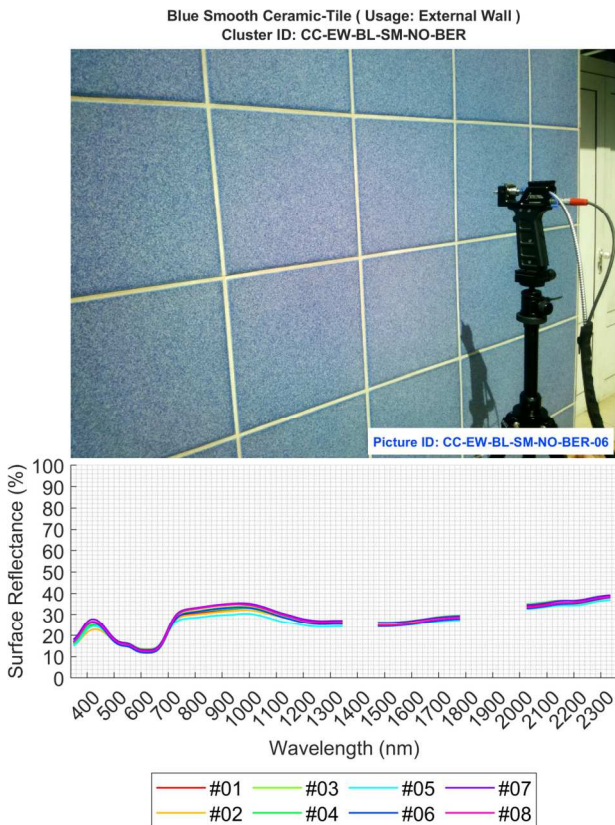


Fig. 3. Photograph (top) and surface reflectance plot (bottom) of eight individual measurements for the “Blue Smooth Ceramic Tile (Usage: Façade)” cluster. The image displays the setup for the 6<sup>th</sup> measurement of this cluster.

The separation of the HS measurements into clusters is initially carried out in an approximate manner during acquisition, i.e., clusters include measurements of similar (or even the same) materials under different conditions (i.e., location, date, time etc.). Afterwards, all the reflectance spectra within a cluster are compared with each other using the Spectral Angle (SA) as a metric:

$$SA(\vec{r}_x, \vec{r}_y) = \text{acos}\left(\frac{\vec{r}_x \cdot \vec{r}_y}{|\vec{r}_x| |\vec{r}_y|}\right) \quad (7)$$

where  $\vec{r}_x$  and  $\vec{r}_y$  are the vector forms of the reflectance spectra x and y respectively, for the valid wavelengths. After experimenting with various thresholds, the 0.10 threshold was identified as the optimal value for SA. Choosing lower values would result in splitting similar HS measurements into different clusters, while higher values would permit distinct HS measurements to be grouped within the same cluster.

In case an element has SA larger than 0.10 compared to other elements of the same cluster, it is removed and its' SA is compared to the spectra of the other clusters. In case the removed element presents SA lower than 0.10 compared to all other clusters, then its assignment in the initial cluster is reviewed. If the material at hand presents similarities with other materials of the cluster, then it is added to this cluster, otherwise a new cluster is created for this element. At the end of this process, all the features that belong to one cluster have SA less than 0.10 with each other. Following this initial intra-cluster comparison process, the individual spectra of materials within a cluster are compared to the rest of the clusters.

The second step of the clustering process includes the evaluation of the maximum intra-cluster SA's. Considering two clusters, cluster C1 with spectrums A, B and C and cluster C2 with spectrums D, E and F. In case, the SA between the spectrums A and B, is higher than the SA between A and D, it is concluded that spectrum A does not belong to the cluster C1. If the maximum SA between spectrum A and the spectra belong to the cluster C2 is lower than the minimum SA between spectrum A and the spectra belong to cluster C1, then its' inclusion in cluster C2 is being reviewed again. If the measured material with spectrum A is the same type (i.e. asphalt) as those included in the cluster C2, it is added to that cluster. In any other case, a new cluster is created for this element. After this cross-check for all elements in all clusters, all the spectra that belong to different clusters have SA values less than 0.10 compared to each other and lower SA compared to any other spectrum of any other clusters.

### III. RESULTS: SPECTRAL LIBRARY STATUS

The methodology (Section II) has been applied to measurements in Berlin (Fig. 1) to measure 284 façade and vertical surfaces. The data are organized in 86 clusters. Spectra in the same cluster contains the same information about the materials type, color, structure, status, usage and cluster ID but, different measurement ID, geo-location, local time, picture, spectral reflectance, spectral incoming and outgoing radiation. Table I. shows a sample of 9 clusters of the HS library, while Fig. 4 shows the image of the first measurement in each cluster, respectively.

### IV. CONCLUSIONS

In this study, an urban hyperspectral library was developed using the Spectral Evolution RS-3500. The library contains 284 hyperspectral measurements in total (façade and vertical), organized in 86 different clusters, for different materials can be found in the city of Berlin. The data are processed to contribute into the *urbisphere* hyperspectral library, which will be used for modelling and other urban environment applications, to help investigate intra- and inter-city variability.

TABLE I. MATERIAL CHARACTERISTICS AND CLUSTER IDS

Material	Usage	Color	Structure	Status	Cluster ID	# Of Samples
(a) Stone	Pavement	Grey	Paver-Blocks	Weathered	ST-PA-GY-PB-WE-BER	6
(b) Granite	Pavement	Black	Plate	Not-Specified	GR-PA-BK-PL-NO-BER	1
(c) Sand	Ground	Grey	Uneven	Not-Specified	SA-GR-GY-UN-NO-BER	3
(d) Asphalt	Ground	Grey	Fine-Roughness	Not-Specified	AS-GR-GY-FR-NO-BER	7
(e) Painted-Asphalt	Ground	Green	Smooth	Weathered	PA-GR-GR-SM-WE-BER	2
(f) Painted-Asphalt	Ground	Red	Smooth	Weathered	PA-GR-RE-SM-WE-BER	3
(g) Ceramic-Tile	External Wall	Blue	Smooth	Not-Specified	CC-EW-BL-SM-NO-BER	8
(h) Brick	External Wall	Black	Smooth	New	BR-EW-BK-SM-NE-BER	2
(i) Brick	External Wall	Orange	Smooth	Weathered	BR-EW-OR-SM-WE-BER	3

Table I. Examples of the clusters included in the *urbisphere* HS library. Each cluster contains a unique 13-digit Cluster ID. All the measurements that belong to the same cluster contain the same information about the material, usage, color, structure, status and cluster ID. Each measurement contains a unique 15-digit measurement ID, which is a combination of the cluster's ID and the measurement's index inside this cluster. For example, the measurement ID for the second entry of the cluster ST-PA-GY-PB-WE-BER is ST-PA-GY-PB-WE-BER-02



Fig. 4. Examples of materials included in the HS library, collected from the area of Berlin. (a) Stones, (b) Granite, (c) Sand, (d) Asphalt, (e-f) Painted-Asphalt, (g) Ceramic-Tiles, (h-i) Bricks. More information about the materials shown in this figure can be found in Table I. The labels show measurements from four neighborhoods in Berlin, color-coded as follows: red for Charlottenburg, yellow for Neukolln, green for Lichtenberg: green, blue for Mitte.

#### ACKNOWLEDGMENT

This work is part of the *urbisphere* project ([www.urbisphere.eu](http://www.urbisphere.eu)), a synergy project funded by the European Research Council (ERC-SyG) within the European Union's Horizon 2020 research and innovation program under grant agreement no. 855005. The article reflects only the

authors' views, and the European Union is not liable for any use that may be made of the information contained herein.

#### REFERENCES

- [1] W. L. Filho *et al.*, "Assessing the impacts of climate change in cities and their adaptive capacity: Towards transformative approaches to climate change adaptation and poverty reduction in urban areas in a set of developing countries," *Science of the Total Environment*, vol. 692, 2019, doi: 10.1016/j.scitotenv.2019.07.227.
- [2] S. Kottaus, T. E. L. Smith, M. J. Wooster, and C. S. B. Grimmond, "Derivation of an urban materials spectral library through emittance and reflectance spectroscopy," *ISPRS Journal of Photogrammetry and Remote Sensing*, vol. 94, 2014, doi: 10.1016/j.isprsjrs.2014.05.005.
- [3] S. K. Meerdink, S. J. Hook, D. A. Roberts, and E. A. Abbott, "The ECOSTRESS spectral library version 1.0," *Remote Sens Environ*, vol. 230, 2019, doi: 10.1016/j.rse.2019.05.015.
- [4] R. Ielhag, A. Schenk, Y. Huang, and S. Hinz, "KLUM: An Urban VNIR and SWIR Spectral Library Consisting of Building Materials," *Remote Sensing 2019, Vol. 11, Page 2149*, vol. 11, no. 18, p. 2149, Sep. 2019, doi: 10.3390/RS11182149.
- [5] "RS-3500 - Spectral Evolution." <https://spectralevolution.com/products/hardware/field-portable-spectroradiometers-for-remote-sensing/rs-3500/#> (accessed Nov. 06, 2022).
- [6] F. Dell'Endice, J. Nieke, B. Koetz, M. E. Schaepman, and K. Itten, "Improving radiometry of imaging spectrometers by using programmable spectral regions of interest," *ISPRS Journal of Photogrammetry and Remote Sensing*, vol. 64, no. 6, 2009, doi: 10.1016/j.isprsjrs.2009.05.007.
- [7] J. Crisp and B. Elliott, *Introduction to Fiber Optics*. 2005. doi: 10.1016/B978-0-7506-6756-2.X5000-5.
- [8] L. Alkhalifah, *Principles of Remote Sensing*. Taylor & Francis Group, 2010.
- [9] R. Loizzo, C. Ananasso, R. Guarini, E. Lopinto, L. Candela, and A. R. Pisani, "The prisma hyperspectral mission," in *European Space Agency, (Special Publication) ESA SP*, 2016, vol. SP-740.
- [10] H. J. Bierens, "The Nadaraya-Watson kernel regression function estimator," *Topics in Advanced Econometrics*, pp. 212-247, Dec. 1994, doi: 10.1017/CBO9780511599279.011.